CONF-9507167--4

UCRL-JC-121573

Richtmyer-Meshkov Instability Experiments on the Nova Laser from Nonlinear Initial Perturbations

T. A. Peyser
P. L. Miller
P. E. Stry
K. S. Budil
E. W. Burke

This paper was prepared for submittal to the
5th International Workshop on the Physics of Compressible Turbulent Mixing
Stony Brook, NY
July 18-21, 1995

February 1996

DISCLAIMER

Richtmyer-Meshkov instability experiments on the Nova laser from nonlinear initial perturbations*

T.A. Peyser, P.L. Miller, P.E. Stry, K.S. Budil and E.W. Burke

Lawrence Livermore National Laboratory

Livermore, CA 94550

I. INTRODUCTION

We present the results from a series of experiments recently completed on the Nova laser studying the growth of the Richtmyer-Meshkov instability from an initially nonlinear perturbation.[1] These are the first experimental measurements of the time-dependent mixing of materials at a shocked interface from a high-amplitude, short-wavelength perturbation in a high Mach number regime. The experiments were simulated using CALE, a two-dimensional arbitrary Lagrangian-Eulerian hydrodynamics code.[2] The calculations correctly captured the measured growth of the mixing zone from the initial applied perturbation. The simulations also permitted consideration of nonideal effects (e.g. post-shock decompression) required to compare the results of calculation and experiment with theory. Both the experiment and calculations were found to be in good agreement with recent theories for the nonlinear evolution of the instability. [3, 4, 5]

In the linear Richtmyer-Meshkov problem, the instability grows from an perturbation whose initial amplitude a_o is small compared to the

wavelength λ of the perturbation. Shock-induced mixing between two dissimilar materials from a nonlinear initial perturbation is a more general and complex form of the Richtmyer-Meshkov problem. In this more general problem, the amplitude of the perturbation may be comparable to the perturbation wavelength ($a_o/\lambda \approx 1$). Examples of this more general problem include: (i) systems for which the surface finish does not satisfy the conditions of linear theory (especially at short wavelengths) (ii) systems with multiple shocks in which the second shock sees a nonlinear perturbation produced by the first shock and (iii) systems in which the late-time or asymptotic regime is important. Recent potential-flow models of Richtmyer-Meshkov bubbles in the asymptotic regime have suggested a bubble velocity $V_B \approx (1/3\pi)\lambda t^{-1}$ [4, 5]. As discussed below, for the Atwood number of the experiment reported here ($A \approx 0.6$), the spike and bubble penetrations are roughly equal and the mix width for the single mode problem should have a logarithmic time dependence.[6] A rudimentary two-phase model, also discussed below, can be derived for the total mix width (spike and bubbles) producing a similar logarithmic time dependence for the case studied here.

II. DESCRIPTION OF THE EXPERIMENT

The experiments described here used Nova, the world's largest laser, to drive shocks in one of the world's smallest shock tubes — a 2 mm long, 700 μm diameter beryllium tube with a 100 μm wall thickness. Eight beams of the Nova laser with a total energy 18-22 kJ, wavelength 0.35 μm in a 1 ns square pulse were used to irradiate the interior of 3 mm long, 1.5 mm diameter cylindrical gold *Hohlraum*.[7] The miniature shock tube was

mounted over a 700 μm diameter hole made at the center of the side of the *Hohlraum*. The working material of the shock tube consisted of a 500 μm diameter, 300 μm long section of a high-density (1.22 g/cc) brominated polystyrene ablator and a 500 μm diameter, 1900 μm long low-density (0.1 g/cc) carbon resorcinol foam payload. The mounting of the shock tube onto the *Hohlraum* wall was optimized by experiment and calculation to produce a nearly planar shock at the location of the interface. This was necessary not only to avoid diagnostic complications, but also to establish a flow with minimal transverse components which might lead to other instabilities such as the Kelvin-Helmholtz instability and unduly complicate the experiment.[1] Thermal x-ray radiation from the interior *Hohlraum* walls incident onto the exposed brominated polystyrene results in a rapid ablation of material and the generation of a strong shock which travels down the shock tube towards the perturbed plastic-foam interface. A schematic of the *Hohlraum* and the attached shock tube viewed along the cylinder axis of the *Hohlraum* is shown in Figure (1).

A rectilinear sawtooth pattern was machined into the high density plastic with a high initial amplitude (a_O=10 μm) relative to the dominant wavelength (λ=23 μm). The large amplitude-to-wavelength (a_o/λ=0.43) initial perturbation was chosen so that the instability would make an early transition into the nonlinear stage.

High-power laser-driven Richtmyer-Meshkov experiments make it possible to achieve extremely high Mach number flows. At the time the shock is incident on the interface, the Mach number of the flow is approximately 20. This is potentially important since experiments at high

Mach number may exhibit the effects of compressibility more strongly than low Mach number experiments. Another significant feature of these experiments is that the working material in the shock tube remains a solid until it is ionized (fluidized) by the passage of the strong shock. There are thus no membrane effects or comparable problems as encountered in shock tubes in which the initial state of the material is a gas or a liquid. In the present study, the perturbation on the high density plastic was characterized with a scanning electron microscope at 200, 1000 and 3000 times magnification. A novel x-ray tomographic microscopy diagnostic using synchrotron radiation from the Stanford Linear Accelerator confirmed that the fully assembled shock tube targets retained their expected structure.[8]

The mixing region width was measured with high-speed gated x-ray framing camera diagnostics using radiography side-on to the shock tube cylinder axis.[9] Two beams of the Nova laser with a total energy of 8-10 kJ at 0.53 μm were focused on a 3 mm square, 25 μm thick titanium foil placed 4 mm from the beryllium-walled shock tube and used to generate the x-ray backlighter source at 4.7 keV. Bromine was added to the high density plastic ablator in a two percent atomic concentration to provide an opacity contrast with the more transparent carbon foam. The intensity of the x-ray transmission from the backlighter and through the experimental shock tube is a function of the densities, opacities, path length and mixture fractions of the two materials. In the absence of instability and mix , the interface between the two regions appears as a sharp transition in the x-ray transmission spatial profile. In the presence of instability and mixing, however, the difference in the relative proportions of each material

through the mixing region results in a more gradual variation in the x-ray transmission as a function of position.

III. EVOLUTION OF THE INSTABILITY

The evolution of the instability can be seen directly in the 2D CALE numerical simulation of the problem. Figure (2) displays a temporal progression of the density and material contour at 2.5, 3.4 ns, 5.0 ns, and 7.5 ns for the sawtooth perturbation. In Fig. (2a), the shock has moved from the origin to a position at 225 μm. The interface between the high and low density materials is located to the right of the shock at 300 μm. Figure (2b) shows the shock incident on the interface at 3.4 ns. The shock pressure at this time is approximately 70 Mbar. The perturbations have begun to invert. In Fig. (2c) at 5.0 ns, growth of the Richtmyer-Meshkov instability into the nonlinear regime is evident from the spike-and-bubble structure. The density and material contours in Figs (2c) and (2d) have been magnified compared to Figs. (2a) and (2b) to permit closer examination of these nonlinear features. In Fig. (2d) at 7.5 ns, there are pronounced roll-ups on the edges of the spike and bubble structures indicating further the evolution of the instability into the nonlinear phase. At 10.0 ns. the instability is far into the nonlinear regime and the boundary between the two materials is highly convoluted as seen in Figure (3b) below.

We compared the shape (or profile) of the interface for the perturbed and smooth target cases for both experimental data and data obtained from numerical simulations. There was a marked difference in the interface

profile for the smooth and perturbed target in the 2D CALE density and material contour simulations at 10 ns . Figure (3a) shows the density plots from a 2D CALE simulations of a smooth (unperturbed) target at 10 ns. Figure (3b) gives the density from a 10 μm amplitude sawtooth (perturbed) target at 10 ns. The images in Figure (4) are the corresponding simulated radiographs of the smooth and perturbed targets at the same time. The simulated radiographs were produced assuming a spatially-uniform x-ray source at 4.7 keV, i.e. the same energy of the actual titanium x-ray backlighter. There were substantial differences in the x-ray transmission across the nominal interface between the two target types. For the smooth (unperturbed) target, there is a sharp discontinuity in the x-ray transmission across the material interface in Fig. (4a) due to the large difference in opacity and the lack of mixing between the two materials. By contrast, for the sawtooth (perturbed) target in Fig. (4b), the slope of the x-ray transmission with position is more gradual indicating mixing (or interpenetration) of the two materials. A more quantitative analysis was made by considering a horizontal average of the transmission values taken over a 100 μm wide region at the center of the simulated radiograph. The total spatial extent of the mixing region was given in terms of the 5-95% transmission levels.

A similar comparison between radiographs of smooth and perturbed interfaces can be observed in the experimental data as well. In the experimental radiographs of the smooth (or unperturbed) target taken up to 15.0 ns (11.2 ns after the shock was incident on the interface), both the shock and interface are clearly visible. The radiographs of the sawtooth (or perturbed) targets taken over the same times show a sharp jump in the

transmission at the shock front, but no such sharp discontinuity at the nominal interface location. Figure (5) gives a 100 μm wide vertical lineout through the center of experimental radiographs from a smooth target taken at 14.8 ns (top) and a sawtooth target taken at 9.2 ns (bottom). In the case of the smooth or unperturbed target, the lineout shows that the interface is still sharp — its width is approximately equal to instrument resolution of the x-ray framing camera (≈15 μm).[9] By contrast, the interface width from the perturbed targets is many times the instrument resolution. Using the 5-95% criterion, we found the mixing region width for the perturbed target is 72 μm. Similar analysis of lineouts for images taken at 7.1, 9.8 ns and 12.1 ns gave mix widths of 48 μm, 59 μm and 77 μm respectively. The greater noise in the smooth target lineout is an artifact of an earlier, noisier gated x-ray framing camera than the instrument used in obtaining the perturbed target data.[9]

IV. COMPARISON OF EXPERIMENTAL RESULTS WITH THEORY

Before the experimental mix width measurements described above can be fruitfully compared with theory, we must first consider if there are any nonideal effects in the experiment which could undermine such a comparison at this stage. Lateral and axial decompression of the materials are unavoidable effects in high-power laser-driven experiments. The lateral decompression of the target is a consequence of the extremely high pressures achieved in the experimental package, but its effects can be minimized by a special mounting of the shock tube to the *Hohlraum* and by tamping the lateral flow with the beryllium wall of the shock tube. The

axial decompression of the target is a consequence of two phenomena not present in idealized theoretical treatments of the problem — the short duration of the drive source relative to the overall experiment as well as reflected rarefactions from the interface. At late times relative to the duration of the laser drive in the *Hohlraum*, there will be significant axial decompression of the material behind the advancing shock wave including the putative mixing region. Since we are interested in following the flow well beyond the point at which the shock imparts an instantaneous velocity to the perturbed interface, we must consider this problem of axial target decompression. The apparent growth of the mix region will be affected by the rarefaction behind the initial shock. If one neglects the axial decompression present in such problems and attempts to compare uncorrected experimental data with theory, the growth of the mix region will appear to be larger than that due solely to the actual hydrodynamic instability.

The relative contribution of axial target decompression to the evolution of the mixing region width was estimated with additional numerical simulations. Calculations of density-matched tracer-layers were carried out with LASNEX and CALE to determine the axial decompression in the problem.[10] We studied the expansion of 10, 20, 40 and 80 μm regions centered about the unperturbed interface location. A separate tracer-layer experiment was designed and carried out using a 300 μm diameter, 125 μm thick opaque silicon dioxide aerogel tracer layer with a density 0.1 g/cc.[11] The 300 μm thick brominated plastic ablator was replaced with 200 μm brominated plastic and 200 μm unbrominated plastic. The silicon dioxide tracer was placed in a counterbore into the low density (0.1 g/cc)

carbon foam at the location of the interface. Both LASNEX and CALE calculations were made of the silicon dioxide tracer layer. The results of these calculations were in good agreement with the measurements suggesting that the axial decompression was being properly simulated by the codes. A decompression factor was determined from the calculations and then divided out of from the measured mix width results from the perturbed sawtooth targets. Figure (6) shows the measured and calculated mix widths from the experiment and from numerical simulations with and without the decompression correction. The diamonds are the mix widths from the 2D CALE calculation and the circles are the mix widths from the experimental data. The grey data points are the raw data; the black data points are corrected for the effect of decompression. The resulting corrected mixing region thickness can be compared to recent potential-flow theories for spike and bubble growth from a single-wavelength perturbation. As noted earlier, these theories suggest that the asymptotic velocity of a single-mode Richtmyer-Meshkov bubble has an inverse time dependence.[4,5,12] At the intermediate post-shock Atwood number of 0.6 as in the present experiment, the penetration of the spikes and bubbles is approximately equal. The nonlinear evolution of the mix width will be therefore logarithmic in time. A single equation for the total mix width (spikes and bubbles) can be derived from a two-phase flow model giving a similar logarithmic time dependence. We begin with the equation of motion for a bubble of low density ρ_p displacing a heavier fluid of density ρ_c

$$V\left(\frac{\rho_c \Delta_A}{2}+\rho_p\right)\frac{dU}{dt}=F_a-AC_d\rho_c U^2 \qquad (1)$$

where V is the volume of the bubble, $\Delta_A/2$ is the added mass coefficient, A is the frontal area ($=\pi d^2/4$ for bubble of diameter d) and C_d is the coefficient of drag. From dimensional analysis $A/V=L^{-1}$, we then assume L=constant=λ (single mode assumption). In the high velocity limit, the added mass coefficient $\Delta_A/2$ is equal to one. Finally we assume further that there are no additional forces (gravity, pressure gradient terms etc.) acting on the system. Eq (1) then becomes

$$\frac{dU}{dt} = -\frac{C_d}{\lambda}\left(\frac{\rho_c}{\rho_c+\rho_p}\right)U^2 \qquad (2)$$

Eq. (2) can be re-arranged to give

$$\frac{dU}{U^2} = -\frac{C_d}{\lambda}\left(\frac{\rho_c}{\rho_c+\rho_p}\right)dt \qquad (3)$$

Integration of Eq. (3) and some algebraic simplification for $t_1=t$, $U_1=U$ and $t_0=0$ leads to the following expression for the bubble velocity

$$U = \frac{U_0}{1+U_0 mt} \qquad (4)$$

where

$$m = \frac{C_d}{\lambda}\left(\frac{\rho_c}{\rho_c+\rho_p}\right) \qquad (5)$$

Finally, integrating Eq. (4) gives

$$a = a_0 + \frac{1}{m}\ln[1 + mU_0(t - t_0)] \qquad (6)$$

where a_0 is the initial amplitude, m is given by Eq. (5) above and depends on the coefficient of drag, the densities of the material and the wavelength of the perturbation, U_0 is the initial relative velocity of the two materials after the passage of the shock and t_0 is the time at which the nonlinear phase of the instability begins. Using the values a_0=10 μm, U_0= 25 μm/ns and t_0=3.8 ns (consistent with calculation), we find from a least squares fit of the data that the behavior of the measured mixing region admits a logarithmic time dependence with m = 0.037 μm^{-1}. This is consistent with Eq. (5) for wavelengths and densities of interest with an apparent coefficient of drag $C_d \approx 4$ — within a factor of two of typical blunt body values from classical fluid dynamics. Figure (6) shows the mix width given by Eq. (8) plotted with values of the free parameters given above. After removing the effect of decompression, data from both experiment and simulation suggest that the nonlinear growth of the mixing width has a logarithmic time dependence as shown by the dotted line.

In conclusion, we have made the first measurements of the growth of a mixing region produced by the Richtmyer-Meshkov instability from a nonlinear initial perturbation. When the effects of target decompression were removed, the width of the mix region was found to grow

logarithmically with time, supporting recent theories for the nonlinear phase of the Richtmyer-Meshkov instability. [3,4, 5, 6, 12]

ACKNOWLEDGMENTS

The authors wish to thank the operations staff at Nova for their expert technical assistance.

*This work was performed under the auspices of the U.S. Department of Energy by the Lawrence Livermore National Laboratory under Contract No. W-7405-ENG-48.

VI. REFERENCES

1. T.A. Peyser, P.L. Miller, P.E. Stry, K.S. Budil, E.W. Burke, D.A. Wojtowicz, D.L. Griswold, B.A. Hammel and D.W. Phillion, *Phys. Rev. Letters* **75** 2332-2335 (1995).

2. R.T. Barton, "Development of a Multimaterial, Two-dimensional, Arbitrary Lagrangian-Eulerian Mesh Computer Program", in Numerical Astrophysics, p.482-497, ed. J.M. Centrella, J.M. LeBlanc and R.L. Bowers, Jones and Bartlett Publishers, Boston (1985).

3. U. Alon, J. Hecht, D. Mukamel, D. Shvarts, *Phys. Rev. Letters* **72**, 2867-2870 (1994).

4. U. Alon, J. Hecht, D. Ofer, D. Shvarts, *Phys. Rev. Letters* **74**, 534-537 (1995).

5. J. Hecht, U. Alon, D. Shvarts, *Phys. Fluids* **6**, 4019-4030 (1994).

6. S.W. Haan, *Phys. Rev. A* **39**, 5812-5825 (1989).

7. E.M. Campbell, *Lasers and Particle Beams*, **9**, 209-231 (1991).

8. J.H. Kinney et al., *Science* **260** 789-792 (1993).

9. K.S. Budil et al., *Revs. Scientific Instruments* , **67**, 1-4 (1996)

10. G.B. Zimmerman and W.L. Kruer, Comments Plasma Phys., **2**, 51 (1975).

11. H. Louis et al., *Fusion Technology*, **28**, 1833-1837 (1995).

12. R. Clift, J.R. Grace and M.E. Weber *Bubbles, Drops and Particles*, Academic Press, NY (1978), i.e. Eq. (11-74) p. 317

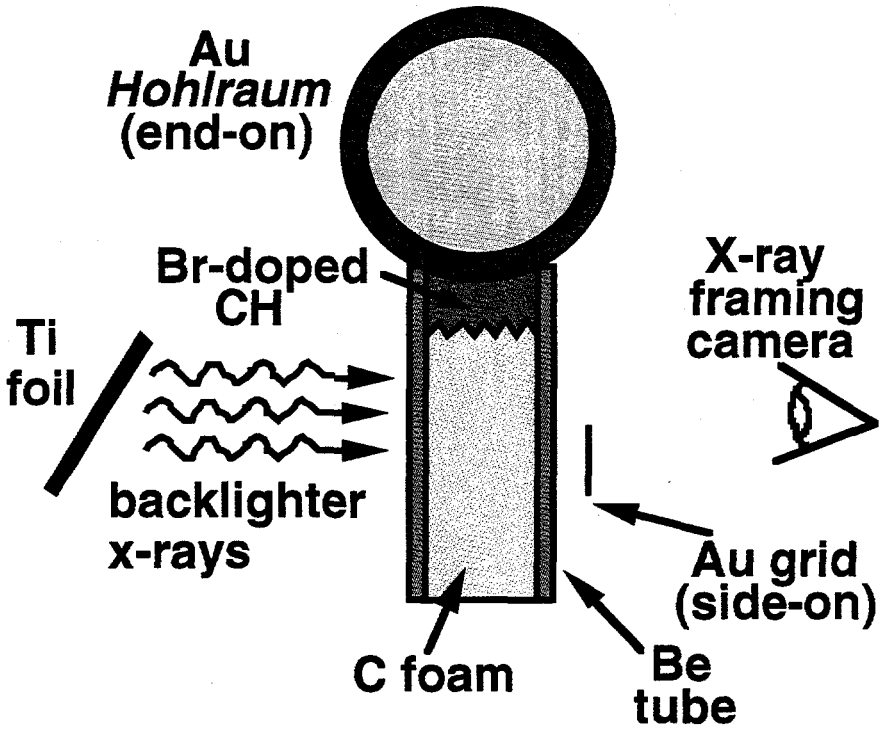

Figure (1): A schematic of the *Hohlraum* and the attached shocktube viewed along the cylinder axis of the *Hohlraum*. Eight beams of the Nova laser were used to irradiate a scale 1 gold *Hohlraum*. The two remaining beams are focussed onto a titanium foil to produce backlighter x-rays for the x-ray framing camera. The beryllium shock tube is 2000 μm long with an outer diameter of 900 μm and a wall thickness of 100 μm. The working material in the shocktube consists of a 300 μm thick high-density, high-opacity brominated plastic ablator followed by a 1700 μm thick low-density, low-opacity carbon foam. The 10 μm amplitude, 23 μm wavelength sawtooth perturbation was machined into the brominated plastic and placed at the interface of the two materials as shown above.

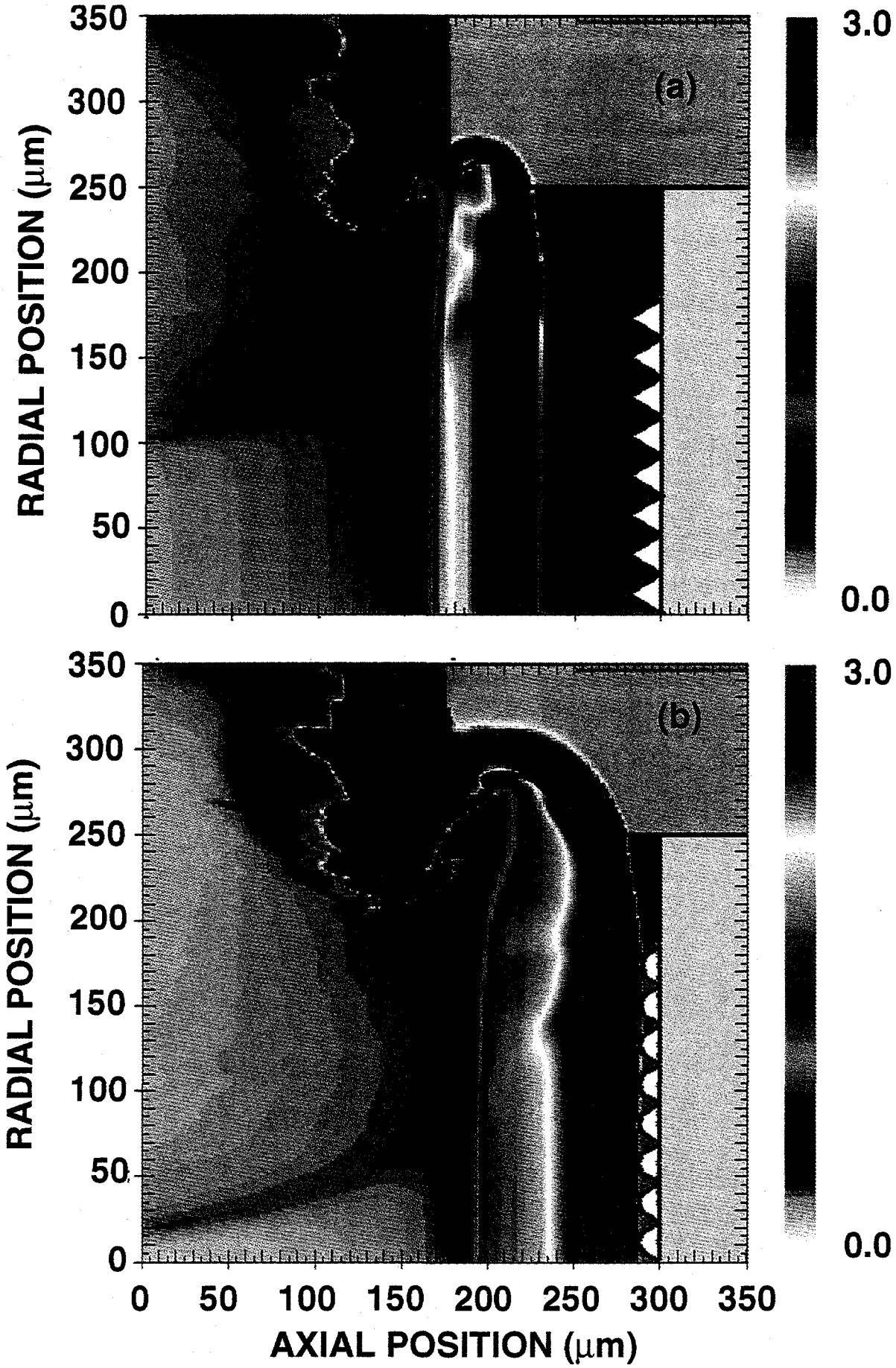

Figure (2): The temporal progression of the density and material contours from 2D CALE numerical simulations at a) 2.5 ns and b) 3.4 ns

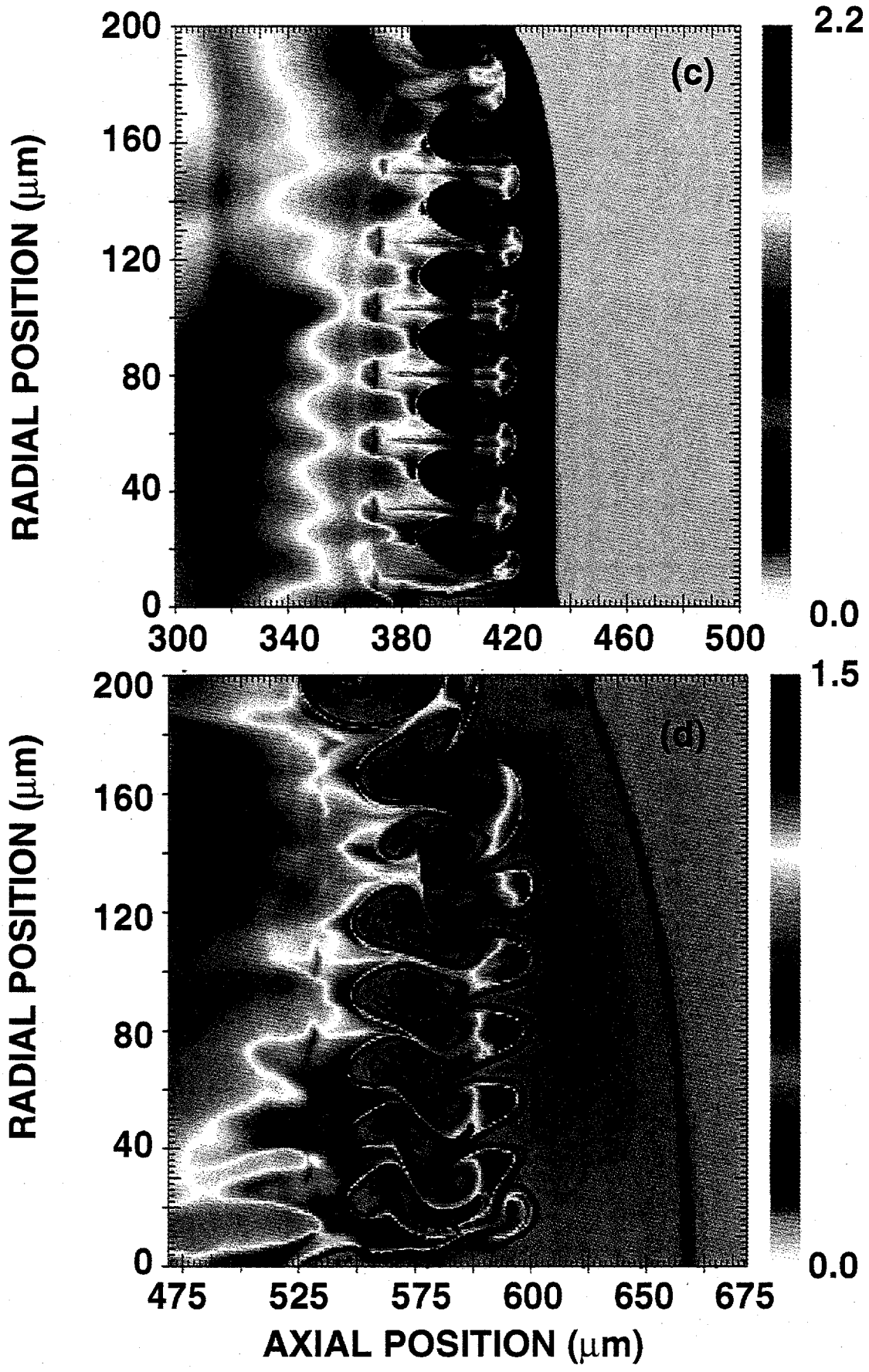

Figure (2): The temporal progression of the density and material contours from 2D CALE numerical simulation at c) 5.0 ns and d) 7.5 ns for the sawtooth perturbation.

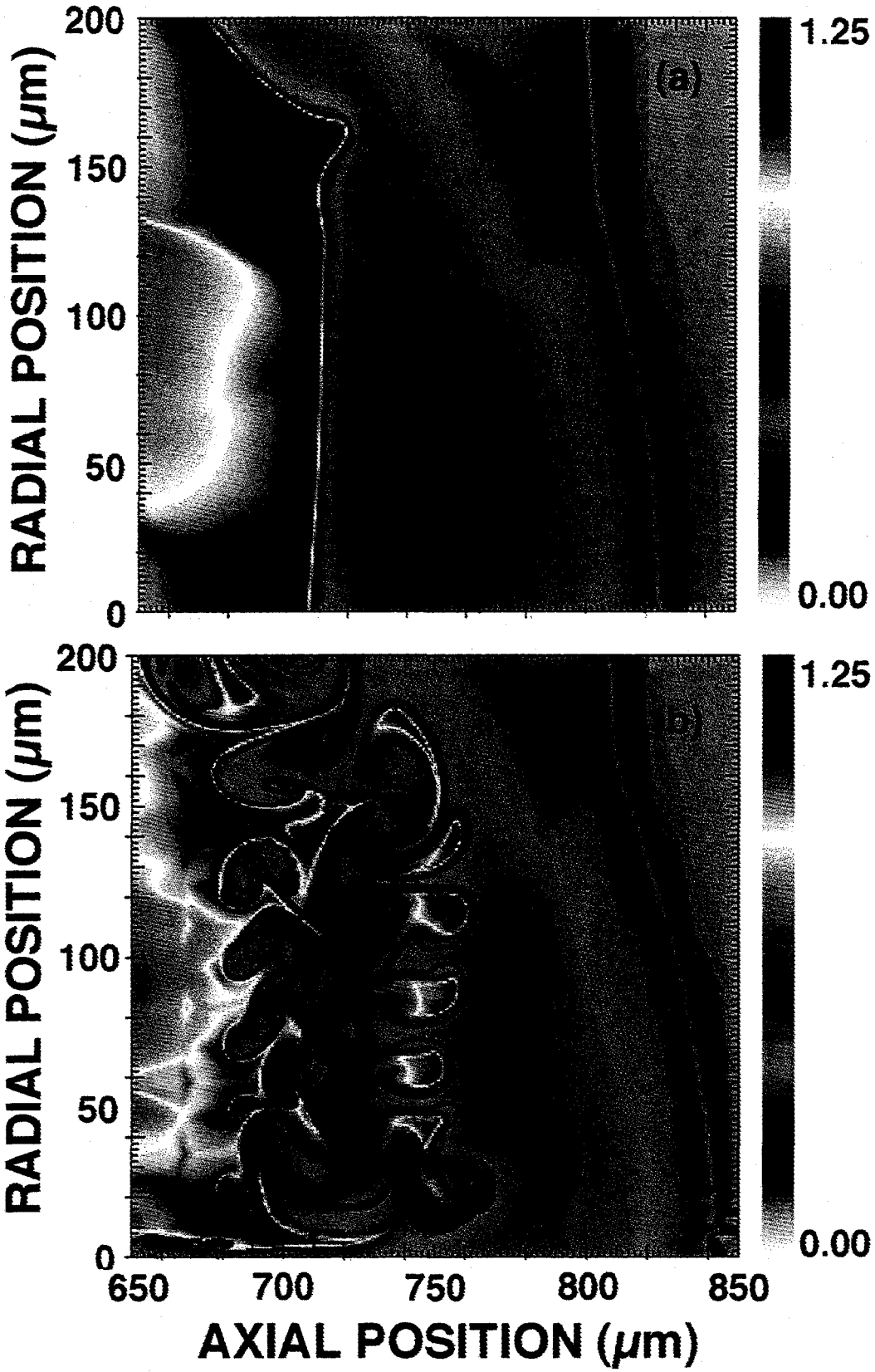

Figure (3): Density and material contours from 2D CALE simulations of smooth (unperturbed) targets and a sawtooth (perturbed) targets at 10 ns. (a) Density plot of smooth target. (b) Density plot of perturbed target.

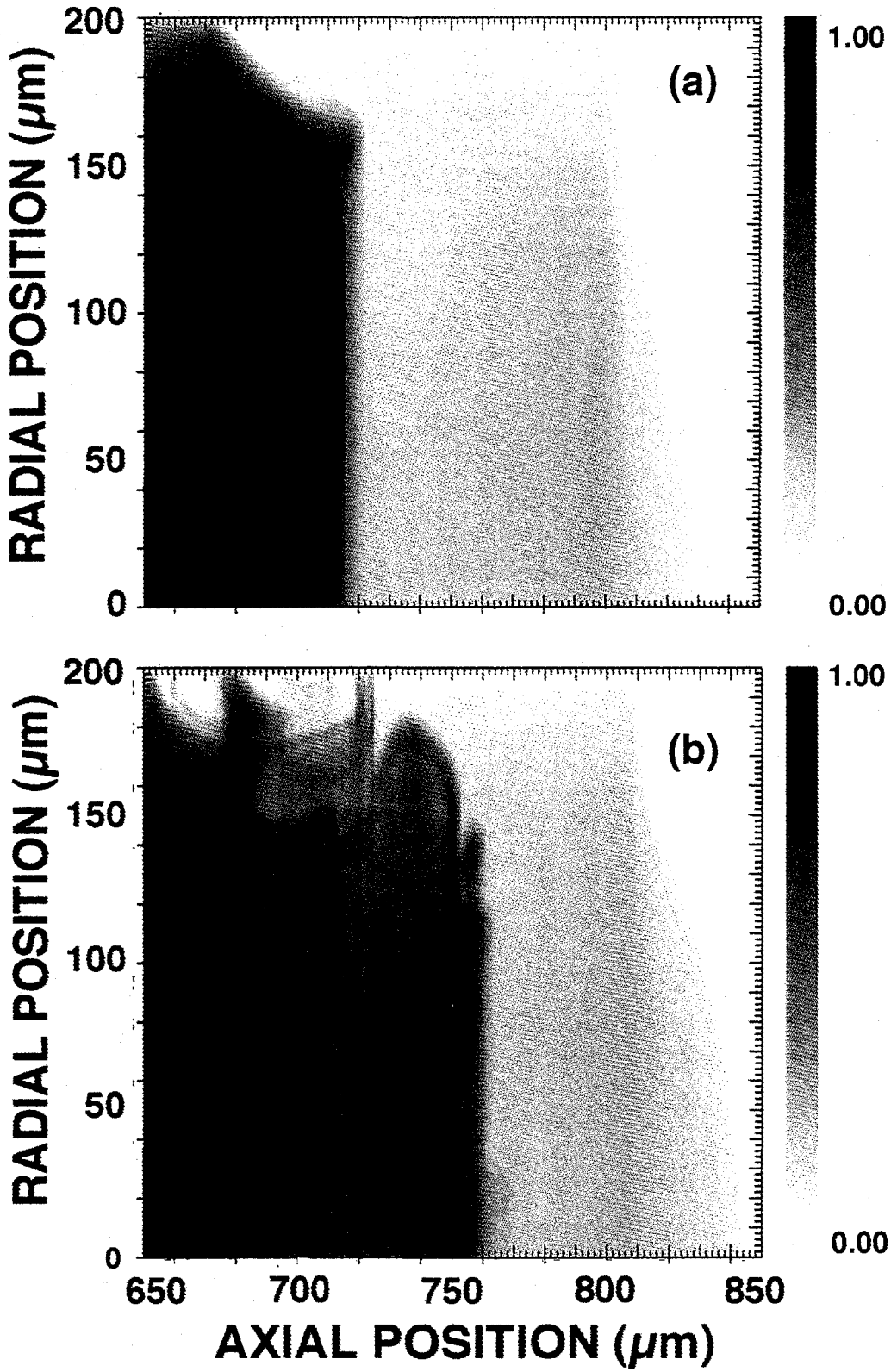

Figure (4): Simulated radiograph from 2D CALE calculation of smooth (unperturbed) targets and a sawtooth (perturbed) targets at 10 ns. (a) Smooth target (b) Perturbed target.

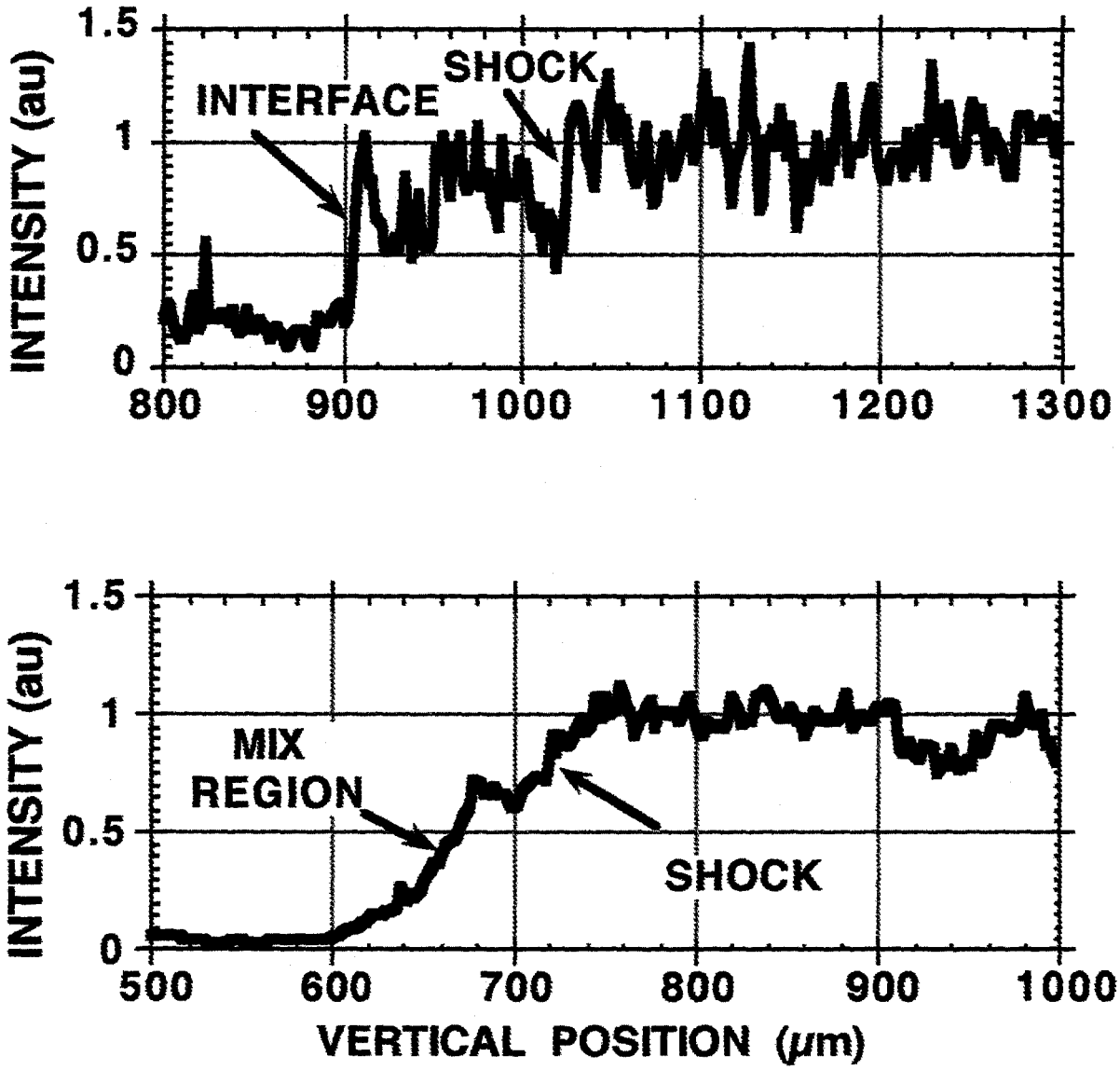

Figure (5): A 100 μm wide vertical lineout through the center of the gated x-ray image of a smooth target at 15.0 ns (top) and the perturbed target at 9.2 ns (bottom).

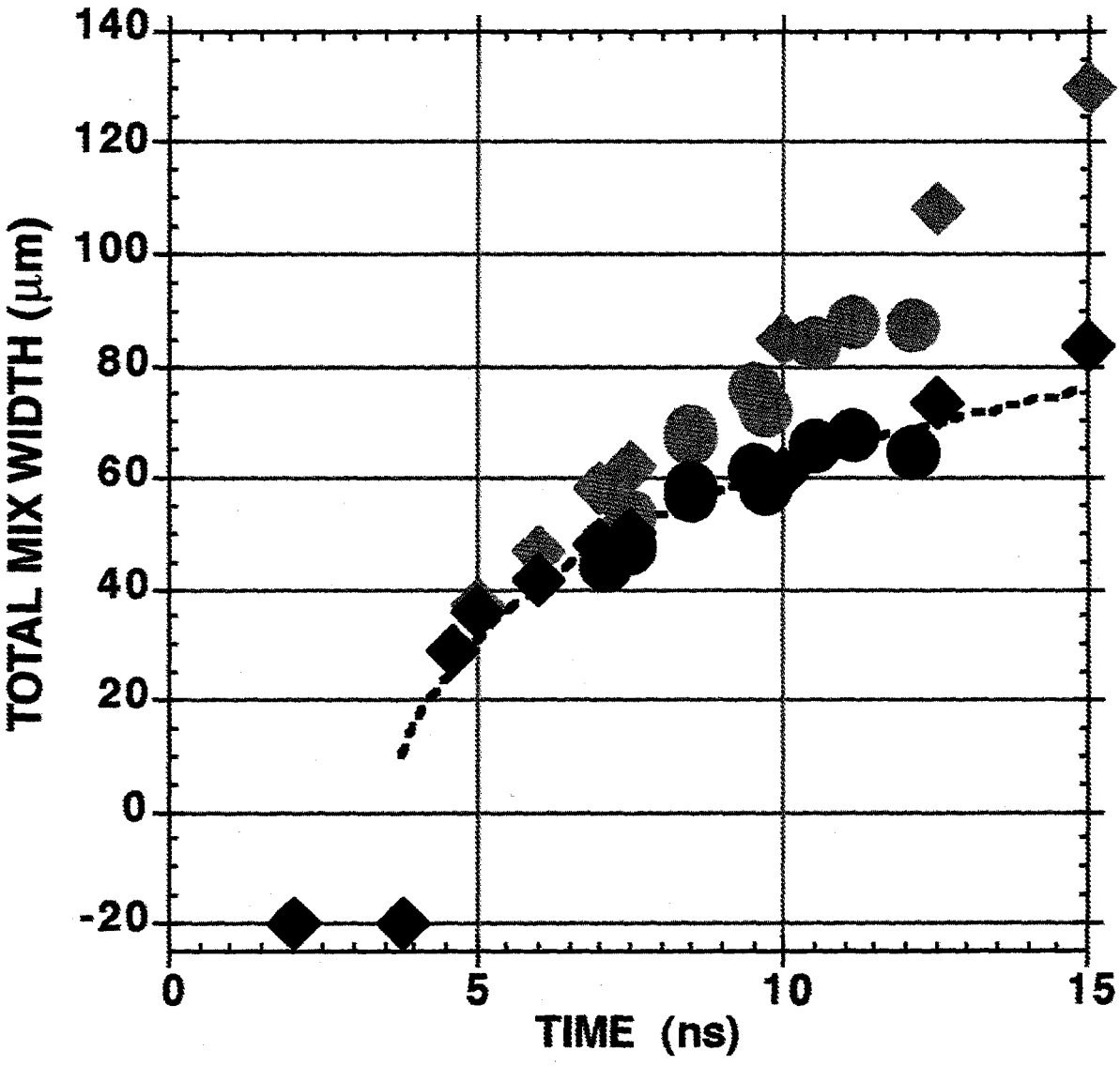

Figure (6) : Measured and calculated mix widths from the experiment and from numerical simulations with and without the decompression correction. The diamonds are the mix widths from the 2D CALE calculation and the circles are the mix widths from the experimental data. The grey data points are the raw data; the black data points are corrected for the effect of decompression. After removing the effect of decompression, data from both experiment and simulation suggest that the nonlinear growth of the mixing width has a logarithmic time dependence as shown by the dotted line.